Hindawi
Scientific Programming
Volume 2022, Article ID 1506627, 10 pages
https://doi.org/10.1155/2022/1506627

Research Article

Mechanical Modeling and Oblique Evaluation of a Full Rotation Steering Tool

Hong Yue,[1] Bo Zeng,[2] Chengxu Zhong,[2] Yezhong Wang,[3] Ye Chen,[2] Xiang Luo,[4] Jun Liang,[4] and Chengyu Xia[5]

[1]*PetroChina Southwest Oil & Gas Field Company, Chengdu, Sichuan 610051, China*
[2]*Shale Gas Research Institute of Petro China Southwest Oil and Gas Field, Chengdu, Sichuan 610051, China*
[3]*Sichuan Shale Gas Exploration and Development Company Limited, Chengdu, Sichuan 610051, China*
[4]*Shentuo (Beijing) Science & Technology Co, Ltd, Daxing District, Beijing 100176, China*
[5]*School of Mechanical Engineering, Yangtze University, Jingzhou, Hubei, 434000, China*

Correspondence should be addressed to Chengyu Xia; qlq1010@126.com

Received 28 March 2022; Revised 29 April 2022; Accepted 16 June 2022; Published 4 August 2022

Academic Editor: Punit Gupta

Directional rotary steerable is one of the key components of modern intelligent drilling, and the analysis of force and deformation in bottom hole assembly is the key to control a well trajectory. Although the introduction of edge calculation will significantly improve the case requirements in engineering application, due to the complexity of directional rotary steerable BHA, such as variable stiffness and discontinuity, few theoretical mechanical models can simultaneously solve the above problems and obtain accurate solutions. In this paper, the inclination angle and diameter of borehole are considered comprehensively. From weight on bit in drilling parameters, assembly structure parameters of multiple variable cross section, discontinuity, stabilizer diameter and position of all sorts of influencing factors, such as the vertical and horizontal bending method combined with the finite element method, a point-type rotary steering BHA is established as a new type of mechanical model, with actual project as an example, through iteration, and the calculated results with the software of numerical verify the correctness of the model. Finally, the model is used to study the bit side force of discontinuous directional rotatory stepping-type BHA, and the effects of offset, weight on bit, and distance between two stabilizers on bit side force are analyzed. The research results provide support for structure optimization and BHA parameter evaluation of directional rotary steerable tools.

1. Introduction

The directional rotary-oriented drilling tool represents the development trend of advanced drilling tools, widely used in the special process. Wells such as ultradeep well, high-difficulty directional well, cluster well, horizontal well, large displacement and branch well are special wells and have high requirements on drilling accuracy, well-hole track quality, drilling speed, and efficiency, making the analysis of discontinuity directional rotary guide drill combination more critical [1–4].

Due to the development of intelligent drilling systems, domestic and foreign research scholars have done a lot of research on the bottom drilling tool combination analysis. In terms of theoretical research, Ebling et al. [5] studied the influence of rotation orientation factors on the yawing force of the bit and proved that the drilling pressure on the yawing force of the bit was not significant. The weighted residual rule of Gao [6] is to improve the calculation accuracy and reduce the workload. It is also applied to the size deflection mechanical analysis of the bottom drill tool combination. Bai Jiaji et al. [7] put forward the famous theory of the vertical and horizontal bending method, which is one of the more accurate solutions [8–11]. Hong et al. [12] put forward a more generalized vertical and horizontal bending method based on the horizontal bending method, which expanded the model established by the original vertical and horizontal bending method. Tikhonov et al. [13] used the central difference algorithm to solve the model when considering the bending

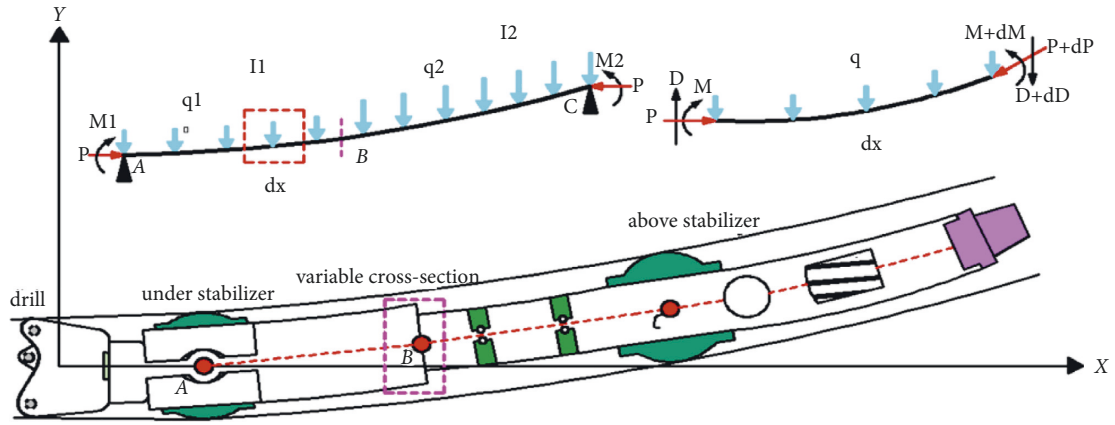

Figure 1: Mechanical model.

stiffness of the drill column, which improves the accuracy of the original calculation. Rublova et al. [14] studied the dynamic characteristics of the drill column by combining the theory of soft rod and rigid rod, thus significantly improving the solution efficiency of the whole well pipe column. Suguira [15] used simplified mathematical equations to optimize the BHA. Feng et al. [16] used finite element simulation to analyze the rotation orientation in terms of finite elements. They proved that the yawing force of the bit was also affected by the good slope. Although it is known that the finite element method is an approximate solution [17–22], Bulent et al. [23] analyzed the intrinsic frequency based on the interaction mechanism of bending and torsion on beams, and the results agree well with experiments.

In conclusion, although the finite element simulation is simple, its modeling is challenging to deal with the nonlinear uncertain contact problem between the noncontinuous section and the final section. Therefore, this paper establishes a theoretical model of discontinuous directional rotary steering drill combination, which can simultaneously solve the multiple stiffnesses, discontinuity, and nonlinear contact problems. Finally, the influence law of each factor on the combination of discontinuous directional rotary guide drills is analyzed by combining with specific instances.

2. Establishment of the Mechanical Model

Figure 1 shows the mechanical model established in this paper. As shown in Figure 1, the combination of discontinuity pointing bottom drill tools is disconnected from the upper and lower stabilizer. The two stabilizers can be regarded as a beam and column subject to vertical and horizontal bending load. Due to the variable cross section between the two stabilizers, the mechanical analysis of the drilling tool combination includes the variable stiffness problem. The microelements were also taken for analysis.

In Figure 1, M_1 and M_2 is bending moment (N · m); m^4, q_1, and q_2 are uniform loads (N/m); and P is axial loading (N). Establishing a plane coordinate system at the drill bit, dx is the microelement section. Take the microelement section (the amplified force map of dx in Figure 1) for mechanical analysis, and establish the balance equation of force on the y-axis.

$$D + dD \; - D + qdx = 0, \tag{1}$$

where D is section shear force (N) and q is uniform load (N/m).

Using the right section, the balance equation of the moment is

$$M - M - dM + Dd\ x + Pdy - \frac{1}{2}qdxdx = 0, \tag{2}$$

where M is bending moment (N · m), P is axial loading (N), and 1/2 $qdxdx$ is the decimal of higher order, and it can be ignored.

$$M = -\mathrm{EI}\frac{\mathrm{d}^2 y}{\mathrm{d}x^2}, \tag{3}$$

where E is modulus of elasticity, Pa, and I is moment of inertia, m4. Formula (4) can be obtained jointly by (1)–(3):

$$\frac{\mathrm{d}^4 y}{\mathrm{d}x^4} + \frac{P}{EI}\frac{\mathrm{d}^2 y}{\mathrm{d}x^2} = \frac{q}{EI}. \tag{4}$$

Formula (4) is the inhomogeneous differential equation and solves its general solution [21]:

$$y = C_1 + C_2 x + C_3 \cos\left(\sqrt{\frac{P}{\mathrm{EI}}}x\right) + C_4 \sin\left(\sqrt{\frac{P}{\mathrm{EI}}}x\right) + \frac{1}{2}\frac{q}{P}x^2. \tag{5}$$

The displacement amount, rotation angle, bending moment value, and shear size are, respectively, given as

$$y = C_1 + C_2 x + C_3 \cos\left(\sqrt{\frac{P}{\mathrm{EI}}}x\right) + C_4 \sin\left(\sqrt{\frac{P}{\mathrm{EI}}}x\right) + \frac{1}{2}\frac{q}{P}x^2\theta \tag{6}$$

$$= C_2 - C_3\left(\sqrt{\frac{P}{\mathrm{EI}}}\right)\sin\left(\sqrt{\frac{P}{\mathrm{EI}}}x\right) + C_4\left(\sqrt{\frac{P}{\mathrm{EI}}}\right),$$

$$\cos\left(\sqrt{\frac{P}{\mathrm{EI}}}x\right) + \frac{q}{P}x, \tag{7}$$

$$M = \mathrm{EI}\left(-C_3\frac{P}{\mathrm{EI}}\cos\left(\sqrt{\frac{P}{\mathrm{EI}}}x\right) - C_4\frac{P}{\mathrm{EI}}\sin\left(\sqrt{\frac{P}{\mathrm{EI}}}x\right) + \frac{q}{P}\right), \tag{8}$$

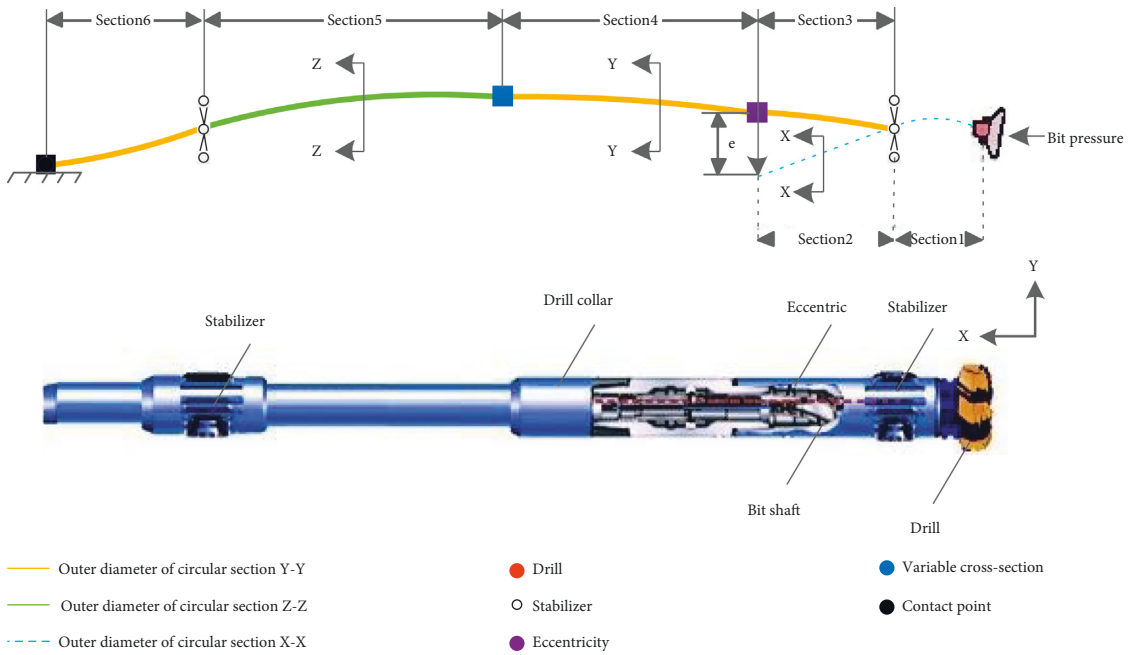

Figure 2: Discontinuous directional rotary guide drilling tool.

$$F = \mathrm{EI}\left(C_3\left(\sqrt{\frac{P}{\mathrm{EI}}}\right)^3 \sin\left(\sqrt{\frac{P}{\mathrm{EI}}}x\right) + C_4\left(\sqrt{\frac{P}{\mathrm{EI}}}\right)^3 \cos\left(\sqrt{\frac{P}{\mathrm{EI}}}x\right),\right. \tag{9}$$

where C_1, C_2, C_3, and C_4 are constant terms.

3. Treatment of the Boundary Conditions

In the discontinuous directional rotation guide, the idea of unit division is used to establish nodes at the intersection of three bars (lower stabilizer), the eccentric ring, the variable section, the upper stabilizer, and the final contact point (as shown in Figure 2). Every two nodes is a section, and using the above formulations (6)–(9) and the continuity condition, the boundary conditions jointly establish the system of equations and then transform into the stiffness matrix.

3.1. The Boundary Conditions at the Drill Bit. In Figure 2, the bit (point A) is hinge with a displacement of 0 and bending moment of 0. $y_{AB} = 0$ and $\mathrm{EI}y''_{AB} = 0$ are obtained by formulas (6) and (8). The matrix form is

$$\begin{bmatrix} 1 & 0 & 1 & 0 \\ 0 & 0 & -k_1^2 & 0 \end{bmatrix} \begin{bmatrix} C_{11} \\ C_{12} \\ C_{13} \\ C_{14} \end{bmatrix} = \begin{bmatrix} 0 \\ -\dfrac{q_1}{p} \end{bmatrix}, \tag{10}$$

where $k_i = \sqrt{p/\mathrm{EI}_i}$, I_i is moment of inertia in section i, q_i is the distribution load in section i, and C_{i1}, C_{i2}, C_{i3}, and C_{i4} are the various coefficients in the equation in section i.

3.2. The Discontinuity Boundary Conditions at the Intersection of Three Bars (Lower Stabilizer). In Figure 2, the lower stabilizer (point B) is located at the intersection of the three rods. The first section, the second section, and the third section both shift to 0 at that point. Moreover, the third section has a bending moment of 0 at that point. According to formulas (6)–(8), $y_{AB} = 0$, $y_{B_1C_1} = 0$, $y_{B_2C_2} = 0$, $y'_{AB} = y'_{B_1C_1}$, $\mathrm{EI}y''_{AB} = \mathrm{EI}y''_{B_1C_1}$, and $\mathrm{EI}\ y''_{B_2C_2} = 0$, and the matrix form is

$$\begin{bmatrix} 1 & l_1 & \cos(k_1l_1) & \sin(k_1l_1) & 0 & 0 & 0 & 0 & 0 & 0 & 0 & 0 \\ 0 & 1 & -k_1\sin(k_1l_1) & k\cos(k_1l_1) & 0 & -1 & 0 & -k_2 & 0 & 0 & 0 & 0 \\ 0 & 0 & -k_1^2\cos(k_1l_1)\mathrm{EI}_1 & -k_1^2\sin(k_1l_1)\mathrm{EI}_1 & 0 & 0 & k_2^2\mathrm{EI}_2 & 0 & 0 & 0 & 0 & 0 \\ 0 & 0 & 0 & 0 & 1 & 0 & 1 & 0 & 0 & 0 & 0 & 0 \\ 0 & 0 & 0 & 0 & 0 & 0 & 0 & 0 & 1 & 0 & 1 & 0 \\ 0 & 0 & 0 & 0 & 0 & 0 & 0 & 0 & 0 & 0 & -k_3^2 & 0 \end{bmatrix},$$

$$\begin{bmatrix} C_{11} \\ C_{12} \\ C_{13} \\ C_{14} \\ C_{21} \\ C_{22} \\ C_{23} \\ C_{24} \\ C_{31} \\ C_{32} \\ C_{33} \\ C_{34} \end{bmatrix} = \begin{bmatrix} -\dfrac{1}{2}\dfrac{q_1}{p}l_1^2 \\ -\dfrac{q_1}{p}l_1 \\ \mathrm{EI}_2\dfrac{q_2}{p} - \mathrm{EI}_1\dfrac{q_1}{p} \\ 0 \\ 0 \\ -\dfrac{q_3}{p} \end{bmatrix}, \tag{11}$$

where B_1C_1 is the second section on the mandrel; B_2C_2 is section 3 on the drill post; and l_i is the length of section i.

3.3. The Discontinuous Contact Conditions at the Eccentric Ring. In Figure 2, at the eccentric ring (point C), because the third and fourth sections on the drill column shift, the angles and the bending moment are equal, the second section bending moment at the point is 0, and its displacement is equal to the minus offset of the third section displacement. Meanwhile, the sum of the shear of the second and third sections is equal to the shear of the fourth section. According to formulas (6)–(9), $y_{B_2C_2} = y_{C\,D}$,$y'_{B_2C_2} = y'_{C\,D}$, EI $y''_{B_2C_2} = \mathrm{EI}y''_{C\,D}$, $\mathrm{EI}y''_{B_1C_1} = 0$, $y_{B_1C_1} = y_{B_2C_2}$-e, and $\mathrm{EI}y'''_{B_1C_1}$ + EI $y'''_{B_2C_2} = \mathrm{EI}y'''_{C\,D}$, and the matrix form is

$$\begin{bmatrix} 0 & 0 & 0 & 0 & 1 & 0 \\ 0 & 0 & 0 & 0 & l_2 & 0 \\ 0 & 0 & 0 & -k_2^2\cos(k_2l_2) & \cos(k_2l_2) & k_2^3\sin(kl_2)\mathrm{EI}_2 \\ 0 & 0 & 0 & -k_2^2\sin(k_2l_2) & \sin(k_2l_2) & -k_2^3\cos(kl_2)\mathrm{EI}_2 \\ 1 & 0 & 0 & 0 & -1 & 0 \\ l_3 & 1 & 0 & 0 & -l_3 & 0 \\ \cos(k_3l_3) & -k_3\sin(k_3l_3) & -k_3^2\cos(k_3l_3)\mathrm{EI}_3 & 0 & -\cos(k_3l_3) & k_3^3\sin(kl_3)\mathrm{EI}_3 \\ \sin(k_3l_3) & k_3\cos(k_3l_3) & -k_3^2\sin(k_3l_3)\mathrm{EI}_3 & 0 & -\sin(k_3l_3) & -k_3^3\cos(kl_3)\mathrm{EI}_3 \\ -1 & 0 & 0 & 0 & 0 & 0 \\ 0 & -1 & 0 & 0 & 0 & 0 \\ -1 & 0 & k_4^2\mathrm{EI}_4 & 0 & 0 & k_4^3\mathrm{EI}_4 \\ 0 & -k_4 & 0 & 0 & 0 & 0 \end{bmatrix}, \tag{12}$$

$$\begin{bmatrix} C_{21} \\ C_{22} \\ C_{23} \\ C_{24} \\ C_{31} \\ C_{32} \\ C_{33} \\ C_{34} \\ C_{41} \\ C_{42} \\ C_{43} \\ C_{44} \end{bmatrix} = \begin{bmatrix} -\frac{1}{2}\frac{q_3}{p}l_3^2 \\ -\frac{q_3}{p}l_3 \\ \mathrm{EI}_4\frac{q_4}{p} - \mathrm{EI}_3\frac{q_3}{p} \\ 0 \\ \frac{1}{2}\frac{q_3}{p}l_3^2 - e - \frac{1}{2}\frac{q_2}{p}l_2^2 \\ 0 \end{bmatrix}.$$

3.4. The Continuity Contact Condition at the Variable Cross Section. In Figure 2, at the variable section (point D), the fourth and fifth sections shift, and turning angles, bending moment, and shear force are equal. According to formulas (6)–(9), $y_{C\,D} = y_{DE}$, $y'_{C\,D} = y'_{DE}$, $\mathrm{EI}y''_{C\,D} = \mathrm{EI}y''_{DE}$, and $\mathrm{EI}y'''_{C\,D} = \mathrm{EI}y'''_{DE}$, and the matrix form is

$$\begin{bmatrix} 1 & l_4 & \cos(k_4 l_4) & \sin(k_4 l_4) & -1 & 0 & -1 & 0 \\ 0 & 1 & -k_4 \sin(k_4 l_4) & k_4 \cos(k_4 l_4) & 0 & -1 & 0 & -k_5 \\ 0 & 0 & -k_4^2 \cos(k_4 l_4)\mathrm{EI}_4 & -k_4^2 \sin(k_4 l_4)\mathrm{EI}_4 & 0 & 0 & k_5^2 \mathrm{EI}_5 & 0 \\ 0 & 0 & k_4^3 \sin(k_4 l_4)\mathrm{EI}_4 & -k_4^2 \cos(k_4 l_4)\mathrm{EI}_4 & 0 & 0 & 0 & k_5^3 \mathrm{EI}_5 \end{bmatrix},$$

$$\begin{bmatrix} C_{41} \\ C_{42} \\ C_{43} \\ C_{44} \\ C_{51} \\ C_{52} \\ C_{53} \\ C_{54} \end{bmatrix} = \begin{bmatrix} -\frac{1}{2}\frac{q_4}{p} l_4^2 \\ -\frac{q_4}{p} l_4 \\ \mathrm{EI}_5 \frac{q_5}{p} - \mathrm{EI}_4 \frac{q_4}{p} \\ 0 \end{bmatrix}. \tag{13}$$

3.5. The Continuity Boundary Condition at the Upper Stabilizer. In Figure 2, at the upper stabilizer (point E), the fifth and sixth sections shift is zero, and the rotation angle and the bending moment are equal. According to formulas (6)–(8), $y_{DE} = 0$, $y_{EF} = 0$, $y'_{EF} = y'_{DE}$, and $\mathrm{EI}y''_{EF} = \mathrm{EI}y''_{DE}$, and the matrix form is

$$\begin{bmatrix} 1 & l_5 & \cos(k_5 l_5) & \sin(k_5 l_5) & 0 & 0 & 0 & 0 \\ 0 & 1 & -k_5 \sin(k_5 l_5) & k_5 \cos(k_5 l_5) & 0 & -1 & 0 & -k_6 \\ 0 & 0 & -k_5^2 \cos(k_5 l_5)\mathrm{EI}_5 & -k_5^2 \sin(k_5 l_5)\mathrm{EI}_5 & 0 & 0 & k_6^2 \mathrm{EI}_6 & 0 \\ 0 & 0 & 0 & 0 & 1 & 0 & 1 & 0 \end{bmatrix},$$

$$\begin{bmatrix} C_{51} \\ C_{52} \\ C_{53} \\ C_{54} \\ C_{61} \\ C_{62} \\ C_{63} \\ C_{64} \end{bmatrix} = \begin{bmatrix} -\frac{1}{2}\frac{q_5}{p} l_5^2 \\ -\frac{q_5}{p} l_5 \\ \mathrm{EI}_6 \frac{q_6}{p} - \mathrm{EI}_5 \frac{q_5}{p} \\ 0 \end{bmatrix}. \tag{14}$$

3.6. The Boundary Condition of Drill Columns Makes Contact with the Well Wall. In Figure 2, at the contact with the drill wall (point F), the angle is 0, the displacement is the well-eye diameter minus the outer diameter of the drill column and then is divided by 2. According to formulas (6)–(8) (y), $y'_{EF} = 0$ and $y_{EF} = d_2 - d_1/2$, and the matrix form is

$$\begin{bmatrix} 0 & 1 & -k_6 \sin(k_6 l_6) & k_6 \cos(k_6 l_6) \\ 1 & l_6 & \cos(k_6 l_6) & \sin(k_6 l_6) \end{bmatrix} \begin{bmatrix} C_{61} \\ C_{62} \\ C_{63} \\ C_{64} \end{bmatrix} = \begin{bmatrix} -\frac{q_6}{p} l_6 \\ \frac{d_2 - d_1}{2} - \frac{1}{2}\frac{q_6}{p} l_6^2 \end{bmatrix}, \tag{15}$$

where d_1 is the diameter of the well-eye (mm) and d_2 is drilling column outer diameter (mm). Because the length of the final segment is unknown, it is difficult to accurately model it with finite elements.

According to the idea of combining finite elements, the constraint equations of the whole drill combination are combined together to form unified mechanical equations of discontinuous directional rotary guide bottom drill combination. It contains a linear matrix equation and a nonlinear equation:

$$AX = B, \tag{16}$$

where

$$A = \begin{bmatrix} A_1 & 0 & 0 & 0 \\ 0 & A_2 & 0 & 0 \\ 0 & 0 & \ddots & \vdots \\ 0 & 0 & \cdots & A_i \end{bmatrix},$$

$$X = \begin{bmatrix} C_1 \\ C_2 \\ \vdots \\ C_i \end{bmatrix}, \tag{17}$$

$$B = \begin{bmatrix} B_1 \\ B_2 \\ \vdots \\ B_i \end{bmatrix}.$$

A_i is the i-point boundary condition matrix, C_i is the coefficient matrix of the i-segment displacement function, and B_i is the constant matrix after the i-point boundary treatment. In this model, it can superposition any variable stiffness and solve the discontinuity problem.

The system of mechanical unity equations of the noncontinuity directional rotation guide bottom drill combination contains a linear matrix equation and a nonlinear equation; therefore, in this paper, the iterative search method is used to solve it. The flow chart is shown in Figure 3.

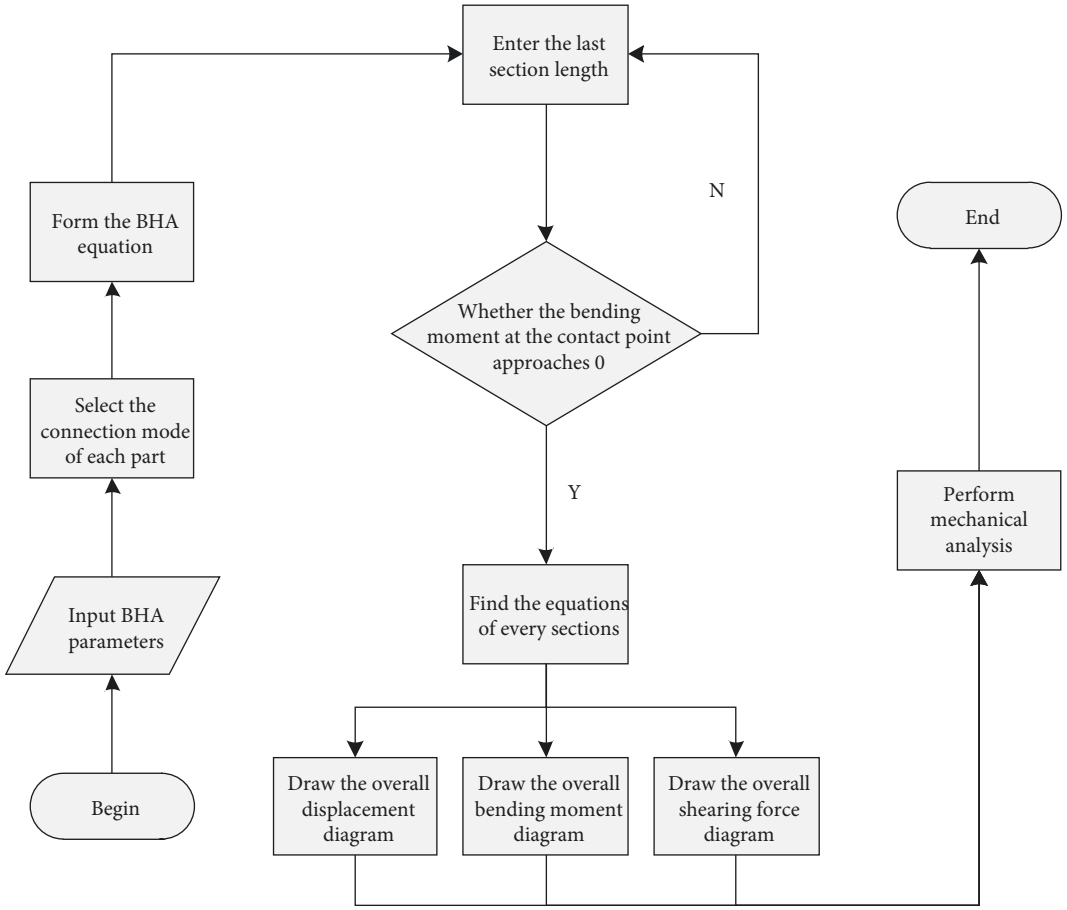

Figure 3: Flow chart.

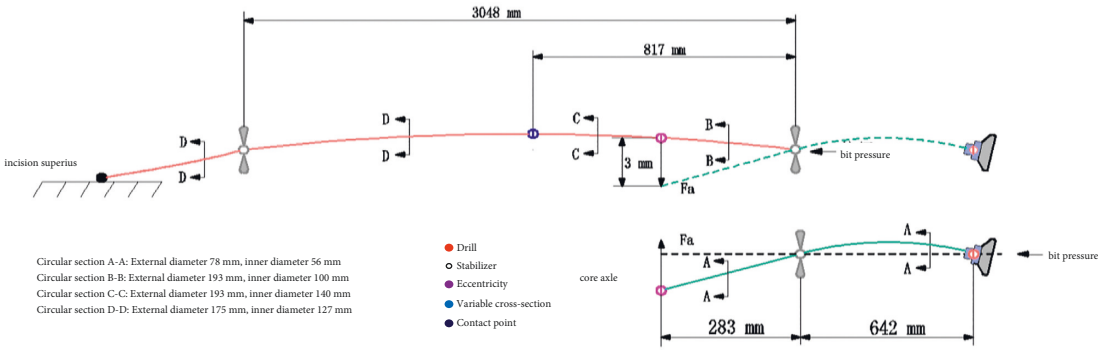

Figure 4: Example of discontinuous directional rotary steering.

4. Application and Verification of Calculation Examples

To validate the correctness of the model, the results of the theoretical model calculation are compared with the results of the literature [9] model (Figure 4). The directional rotary guide drill combination includes variable stiffness and discontinuity problems. The well slope angle is 0 ~ 90, well size is 215.9 mm, drilling pressure is 245 kN, drilling fluid density is 1200 kg/m^3, stabilizer outer diameter is 215.9 mm, the drill tool density is 7 850 kg/m^3, and Young's modulus is 2.06×10^{11} Pa.

The drill bit is the zero point of the two-dimensional coordinate axis, and the offset is negative downward. The value of the bending moment, the displacement, and the shear force are calculated by MATLAB programming software. Figure 5 is the displacement map calculated using the model of literature [9] and the model in this paper (1 is the results of the model of this paper and 2 is the results of the model in literature [9]). The comparison found that the two results are very close. Through the specific values of Figure 4 (lower left corner), the bending moment, displacement amount, and shear force of the bit, upper and lower stabilizer, and variable section are carefully checked so as to verify the correctness of this model.

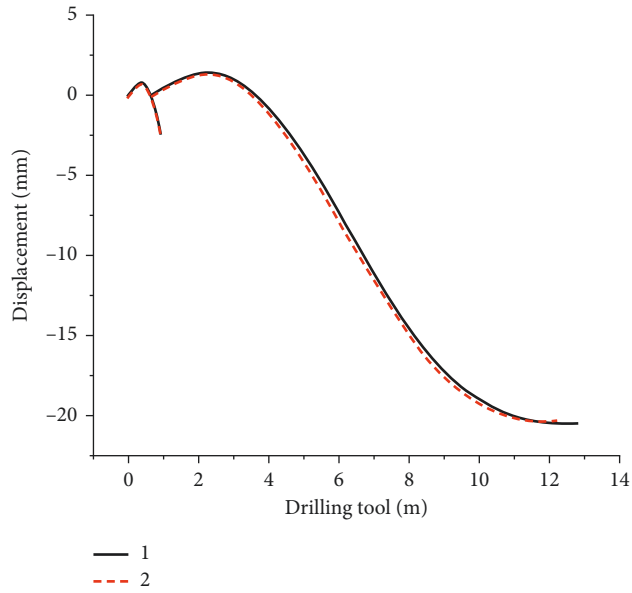

Figure 5: Displacement diagram.

Figure 6: Discontinuous directional rotary guidance.

5. Analysis of Mechanical Properties of the BHA

In this paper, the microelement method, finite element idea, and programming software (MATLAB) are used to establish the discontinuous directional rotation-oriented mechanical analysis software jointly. Based on the above examples, the influence of the various factors on the yawing force of the drill bit was analyzed by the control variable method. The 3-dimensional diagram is as follows (Figure 6).

5.1. Effect of the Offset on the Yawing Force of the Drill Bit. Based on the actual working conditions and the above model, the influence of the offset on the yawing force at the bit is analyzed by changing the offset (e) of the eccentric ring (Figure 7), and the results are shown in Figure 8. When the drill pressure is certain, the drill bit yawing force increases with the offset of the eccentric ring, and the yawing force of the drill bit increases significantly. However, when the offset of the eccentric ring is certain, although the yawing force of the drill bit increases with the drilling pressure, the increase is not obvious. It is concluded that although the drilling pressure and offset both affect the drill bit yawing force, the drilling pressure has little influence. Thus, the offset can be appropriately increased to increase the yawing force of the bit.

5.2. Effect of the Distance to the Bit on the Yawing Force of the Bit. The stabilizer (Figure 9) plays a supporting role in BHA, but its position has a great influence on the mechanical properties of the rotation guide. Figure 10 shows the effect of the distance between the bit and the lower stabilizer on the yawing force of the bit. When other conditions are certain, as

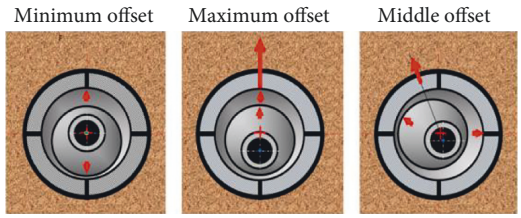

Figure 7: The offset state of the directional rotary guide eccentric ring.

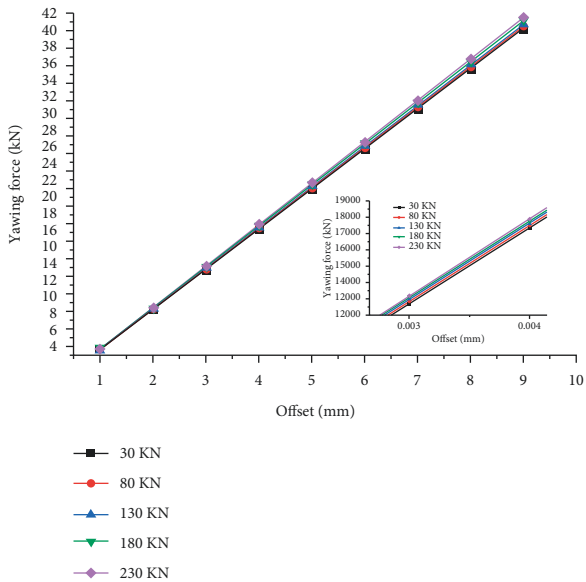

Figure 8: Influence of offsets under different bit pressures on the yawing force.

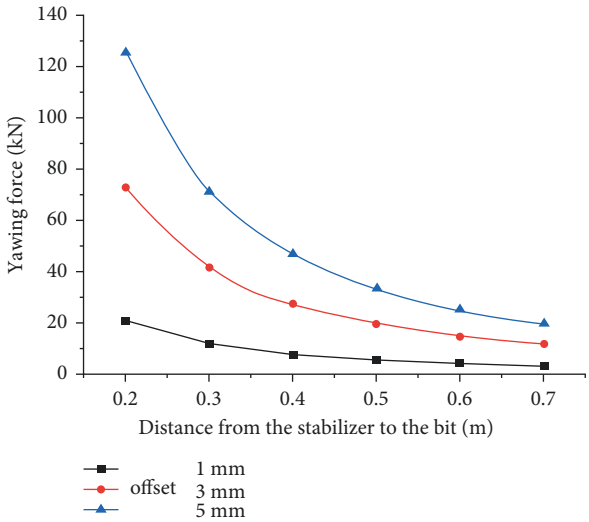

Figure 9: Relationship between bit yawing force and bit distance of the stabilizer.

the distance between the drill bit to the lower stabilizer increases, the yawing force at the drill bit gradually decreases. In the beginning, the decrease is very obvious, and as the distance gradually increases, the decrease becomes more

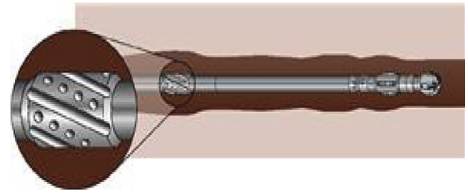

Figure 10: Schematic diagram of the stabilizer.

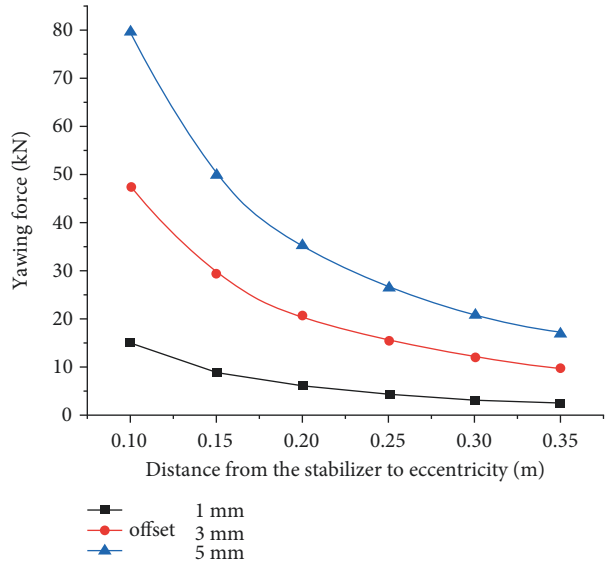

Figure 11: Relationship between yawing force of the bit and distance between the lower stabilizer and eccentricity.

gentle. It is known that appropriately reducing the distance between the lower stabilizer and the bit or increasing the offset can increase the yawing force of the bit.

5.3. Effect of the Distance from the Lower Stabilizer to the Eccentric Ring on the Yawing Force of the Drill Bit. Figure 11 shows the effect of the distance between the lower stabilizer and the eccentric ring on the yawing force of the bit. When other conditions are certain, as the distance from the lower stabilizer to the eccentric ring gradually increases, the yawing force at the bit drops significantly at the beginning, flattening out as the distance gradually increases. In the case of the offset increase, the decline range is more obvious. It is known that the distance between the lower stabilizer and the eccentric ring is appropriately reduced or increases the offset, and a large drill bit yawing force can be obtained.

5.4. Effect of the Distance between the Two Stabilizers on the Yawing Force of the Drill Bit. Figure 12 shows the effect of the distance between the two stabilizers on the yawing force of the bit. Since the two stabilizers contain a variable section, only the distance between the upper stabilizer and the variable section is increased when other conditions exist. The distance between the two stabilizers also increases, and the yawing force at the bit gradually decreases. It is known that

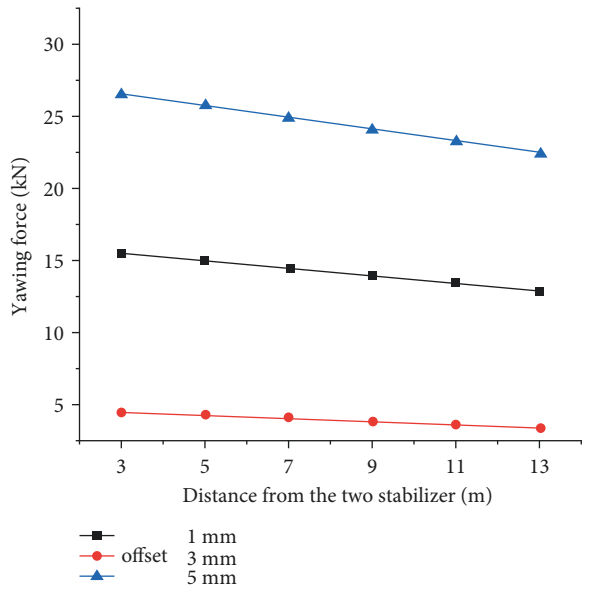

Figure 12: Relationship between the yawing force of the bit and the distance between the two stabilizers.

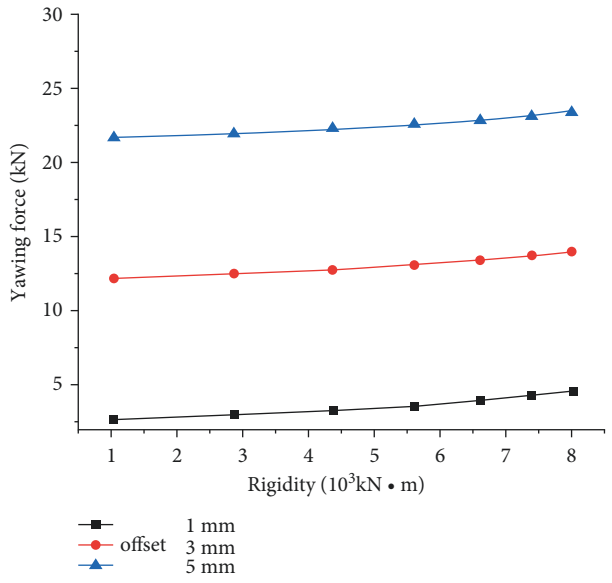

Figure 13: Relationship between stiffness and yawing force of the bit.

appropriately reducing the distance between the stabilizer to the variable section can increase the size of the yawing force of the bit. But still, the impact of the offset on the yawing force of the bit is less.

5.5. Effect of Stiffness on the Yawing Force of the Drill Bit. Taking the stiffness of the last bit as an example, it is clear from Figure 13 that when the difference between the internal and external radius of the previous drill column increases, its stiffness gradually increases, and the yawing force of the drill bit gradually increases with the stiffness. Therefore, the stiffness also affects the yawing force of the bit. The difference between the internal and outer diameter of the last bit should be appropriately increased to improve the yawing force of the bit effectively.

6. Conclusion

According to the microelement method and finite element idea, the combined theoretical model of the discontinuous directional bottom drill is jointly established. It is combined with the programming software (MATLAB) to form the discontinuous directional rotation-oriented mechanical analysis software. Finally, through the theoretical analysis, the model's correctness and the software are verified.

The conclusion is as follows:

(1) By studying the influence of the offset and drilling pressure on the yawing force of the drill bit, the greater the offset of the eccentric ring, the greater the yawing force of the drill bit.

(2) Adjusting the size of the offset in a certain range can control the well-eye track. When the drill pressure increases, the yawing force of the drill bit also increases, but the increase is very small. Therefore, the drilling pressure is not the key factor in increasing the drilling bit's yawing force.

(3) The distance between the bit to the lower stabilizer, the lower stabilizer to the eccentric ring, and the distance between the two stabilizers will all affect the yawing force of the bit.

(4) Although the yawing force of the drill bit decreases with the distance of the three bars, the calculation result shows that the distance from the bit to the lower stabilizer and the lower stabilizer to the eccentric ring greatly affects the yawing force. In contrast, the distance between the two stabilizers has less influence on the yawing force.

(5) To increase the drill bit's yawing force, the distance between the drill bit to the lower stabilizer and the lower stabilizer to the eccentric ring should be appropriately reduced.

Data Availability

The datasets used and/or analyzed during the current study are available from the corresponding author on reasonable request.

Conflicts of Interest

The authors declare no conflicts of interest with respect to the research, authorship, and/or publication of this article.

References

[1] J. Li, X. Ni, and X. Zhang, "Discussion on the design of dynamic directional rotary steering drilling tool," *Oil Field Machinery*, vol. 38, no. 2, pp. 63–66, 2009.

[2] J. Zhang and Z. Yu, "Analysis of deflecting ability of static controllable eccentric rotary steering drilling tool," *Oil Drilling Technology*, vol. 11, no. 5, pp. 45–48, 2000.

[3] Z. Wu, M. Jiang, and Y. Gu, "Direction control and dynamics simulation of bias unit of point-the-bit RSS," *Drilling and Production Technology*, vol. 44, no. 6, pp. 13–18, 2021.

[4] Y. Geng, Z. Song, and W. Wang, "Dynamic toolface measurement for dynamic point-the-bit rotary steerable drilling tool," *Journal of Chinese inertial technology*, vol. 28, no. 3, pp. 323–329, 2020.

[5] B. Ebling, D. Jurcic, K. M. Barac et al., "Influence of various factors on functional dyspepsia," *Wiener Klinische Wochenschrift*, vol. 128, no. 1-2, pp. 34–41, 2016.

[6] S. Fu and D. Gao, "A new algorithm for two dimensional analysis of BHA," *Natural Gas Industry*, vol. 31, no. 8, pp. 62–64, 2004.

[7] Y. Su, X. Tang, and Z. Chen, "Equivalent loading method for solving beam-column with initial bending and its application in drilling engineering," *Mechanics in Engineering*, vol. 26, no. 1, pp. 42–44, 2004.

[8] J. Bai and Y. Su, *Deviation Control in Direction Drilling*, China Petroleum Industry Press, Beijing, China, 1990.

[9] X. Tang, "Non-uniform stiffness beam-column theory andits application," *Mechanics in Engineeting*, vol. 23, no. 5, pp. 12–15, 2011.

[10] J. Bai, "Bottom hole assembly problems solved by beam-column theory," in *Proceedings of the International Meeting on Petroleum EngineeringPaper Presented by Chinese Party*, Beijing, ChinaSPE-10561-MS, Beijing, China, March 1982.

[11] X. Tang, Y. Su, and Y. Ge, "BHA Mechanicalanal-ysis for rotary steering drilling system," *Mechanics in Engineerin-g*, vol. 35, no. 1, pp. 12–15, 2013.

[12] D. Hong, X. Tang, and Y. Su, "Generalized longitu-de-nal-transverse bending method for discontinuous rotary steeri-ng assembly," *J. Journal of Petroleum Sciences*, vol. 35, no. 3, pp. 543–550, 2014.

[13] V. Tikhonov, K. Valiullin, and K Nurgaliev, "Model for stiff string torque and drag," in *Proceedings of the SPE/IADC Drilling Conference,2013*, Dubai, UAE, March 2013.

[14] Y. D. Rublova, A. A. Kityk, N. G. Bannyk, V. Protsenko, and F. Danilov, "The influence of various factors on corrosion of mild steel in deep eutectic solvents," *Materials Today Proceedings*, vol. 6, pp. 232–236, 2019.

[15] J. Sugiura, "Optimal BHA design for steer ability and stability with configurable rotary-steerable system," in *Proceedings of the Paper presented at the SPE Asia Pacific Oil and Gas Conference and Exhibition*, Article ID SPE114599, Perth, Australia, October 2008.

[16] C. Feng and Y. Peng, "Finite element simulation of yawing force of rotating guided drilling tool BHA," *Petroleum Machinery*, vol. 27, no. 9, pp. 14–16, 2006.

[17] A. R. McSpadden, O. D Coker, and G. C. Ruan, "Advanced casing design with finite-element model of effective dogleg severity, radial dis-placements and bending loads," *SPE Drilling and Completion*, vol. 27, no. 3, SPE 141458, 2011.

[18] Y. B. Hu, Q. F. Di, W. Zhu, Z. Chen, and W. Wang, "Dynamic characteristics analysis of drillstring in the ultra-deep well with spatial curved beam finite element," *Journal of Petroleum Science and Engineering*, vol. 82-83, no. 82/83, pp. 166–173, 2012.

[19] Y. Z. Zhang, J. M. Zhang, and Z. J. Shi, "Application and development of numerical simulation for underground horizontal directional drilling," *Journal of Coal Science and Engineering*, vol. 18, no. 1, pp. 101–107, 2012.

[20] J. Weiqi, Z. Zhiliang, and X. Jinrong, "Finite element analysis of coiled tubing forces," *Modern Manufacturing Technology and Equipment*, vol. 4, no. 1, pp. 25-26, 2009.

[21] X. Z. Zhu, Y. D. He, L. Chen, and H. Q. Yuan, "Nonlinear dynamics analysis of a drillstring-bit-wellbore system for horizontal oil well," *Advanced Science Letters*, vol. 16, no. 1, pp. 13–19, 2012.

[22] B. Yardimoglu and D. J. Inman, "Coupled bending-bending-torsion vibration of a pre-twisted beam with aerofoil cross-section by the finite element method," *Shock and Vibration*, vol. 10, no. 4, pp. 223–230, 2003.

[23] C. Xia, Z. Wang, and Y. Fan, *The Mechanical Analysis Method Of Discontinuous Directional Rotary Guided Drilling Assembly*Hubei Province: Patent CN111428384A, 2020-07-17, 2020.